# Configuration Interaction Theory. Effects of Overlapping Resonances*

Frederick H. Mies
*National Bureau of Standards, Washington, D. C.*, 20234
(Received 29 April 1968)

Fano's resonance theory is extended to include the interaction of many resonances with many continua and inelastic couplings between continuum states. In particular a new parameter is introduced; the overlap matrix between the continua to which neighboring resonances are coupled. Resonances which are coupled to the same channel states may be said to overlap. If their widths are comparable to their spacings the resultant effects on photoabsorption or on the scattering matrix can be quite profound. The apparent widths may bear little relation to the widths due to configuration interaction, and the resultant structure may not fit the usual Fano-Buetler profiles for isolated resonances.

The effects of overlapping are examined for various models which are representative of atomic photoabsorption and electron-diatomic molecule scattering. It is demonstrated that without prior knowledge of the overlap matrix it is impossible to uniquely characterize a resonance from limited experimental observations. Scattering and photoabsorption experiments should be designed to examine all possible channels, i.e., both differential and inelastic cross sections. Even so, without the parallel support of theoretical estimates of partial widths, and the signs of the configuration interaction matrix elements, the interpretation of resonance phenomena and in particular the parameters which are extracted must be accepted with severe reservations.

## I. INTRODUCTION

The width of a resonance $\Gamma_n$ is defined as the sum of all its partial widths $\Gamma_{n,\beta}$ into the set of open channels $\{\beta\}$, and is a measure of the configuration interaction (CI) between the resonance state and the continua. For an isolated resonance the CI width may be inferred directly from the experimentally observed width. However, this simple relationship can be destroyed when the widths of adjacent resonances begin to approach or exceed the spacings. Fortunately for a collection of resonances which are coupled to different channels $\beta$, their shapes are merely superimposed and there is no intrinsic problem in analyzing the observations. However, those resonance states which are coupled to the same channels exhibit profound interference effects and are said to "overlap."

Overlapping resonances have been treated and discussed briefly by Fano in connection with a Rydberg series of auto-ionizing atomic lines[1] which consists of many resonances coupled to one continuum. Application of this many resonance–one channel theory to the time dependent behavior of activated, or metastable molecules[2] has demonstrated one extraordinary effect of overlapping, i.e., the extremely nonexponential decay of an overlapped resonance state. The purpose of the present study is to extend Fano's CI theory in two ways. First, since our ultimate purpose is to apply CI theory to molecular scattering where the density of resonance states and channel states makes overlapping inescapable, we must include the case of many resonances coupled to many continua (or channels). Second we introduce inelastic potential scattering between the continua and give more explicit attention to electron scattering cross sections in addition to photoabsorption processes.

Recently Feshbach[3] has presented an extended version of his Unified Theory of Nuclear Reactions which incorporates the effects of overlapping resonances with results which are equivalent to those reported here. However, it is felt that the CI theory is of sufficient interest, and of more explicit application to the analysis of both photoabsorption and electron-scattering phenomena to warrant a detailed development.

We construct the set $\{\alpha\}$ of degenerate, orthonormal $(N_0+1)$-electron continuum wave functions $\Psi_{\bar{\alpha},E}$ at total energy $E$, which describe the interaction of a free electron and a $N_0$-electron atom or molecule M($s$) in quantum state $s$. These wave functions correspond to the continuum states of the $(N_0+1)$-electron system $M^-(\alpha,E)$, i.e., $E \geq 0$, where $E=0$ is the ionization threshold. Our particular concern is with the role of transient $(N_0+1)$-electron "states" $M^-(n)$ which are bound and yet which have approximate eignevalues $E_n \geq 0$ and hence lie within the continua.

If $M$ is a neutral species then $M^-(n)$ are the so-called negative-ion states or resonance states which are "observed" in electron scattering. They influence the asymptotic properties of $\Psi_{\bar{\alpha},E}$ and hence the scattering matrix $S$ which determines the scattering cross sections.

$$e^- + M(s) \xrightarrow{r} \sum_n M^-(n) \qquad (1r)$$

$$\sum_n M^-(n) \xrightarrow{d} \sum_{s'} e^- + M(s') \qquad (1d)$$

The relative proportions of resonance scattering Eq. (1r) vs direct potential scattering Eq. (1d) is of interest.

If M is a positive ion then $M^-(n)$ represents the autoionizing states observed in the photoabsorption and photoionization of the neutral ground-state molecule $M^-(i)$.

$$M^-(i) + h\nu \xrightarrow{a} \sum_n M^-(n) \qquad (2r)$$

$$\sum_n M^-(n) \xrightarrow{d} \sum_s e^- + M(s) \qquad (2d)$$

The final states in the transition $\Psi_i + h\nu \rightarrow \Psi^-_{\alpha,E}$ are the same functions which describe electron scattering by the ion M($s$). The relative prominence and shape of the autoionizing lines Eq. (2r) versus the direct (background) photoionization Eq. (2d) must be extracted from the total photoabsorption cross section, $\sigma_E$,

$$\sigma_E = \sum_\alpha |\langle \Psi^-_{\alpha,E} | T | \Psi_i \rangle|^2 \tag{3}$$

where $T$ is a generalized expression for a transition operator.

The generalized version of the CI theory is presented in the next section. This is an extension of Fano's development and we intentionally follow his format rather closely. Section III discusses the results and shows how they reduce to Fano's previous results in special cases. Models are constructed to exhibit overlapping effects in atomic photoabsorption (Sec. IV) and in electron diatomic molecule scattering (Sec. V). Section VI is devoted to a summary and conclusions.

## II. CONFIGURATION INTERACTION THEORY

### A. Formulation

We start from the assumption that by some previous expansion and partial diagonalization we have on hand subsets of approximate bound $\{\Psi_n{}^0\}$ and continuum $\{\Psi_{\beta,E}{}^0\}$ wave functions which diagonalize separate submatrices of the total Hamiltonian $H$,

$$\langle \Psi_n{}^0 | H - E | \Psi_m{}^0 \rangle = (E_n - E)\delta_{n,m} \tag{4}$$

$$\langle \Psi_{\beta',E'}{}^0 | H - E | \Psi_{\beta'',E''}{}^0 \rangle = (E' - E)\delta_{\beta',\beta''}\delta(E'' - E'). \tag{5}$$

Our task is to introduce the off-diagonal terms which couple the subsets $\{n\}$ and $\{\beta,E'\}$,

$$\langle \Psi_n{}^0 | H - E | \Psi_{\beta,E'}{}^0 \rangle = V_{n,\beta}(E,E') \tag{6a}$$

and to use a linear combination of the two sets to represent the exact total wave function $\Psi^-_{\alpha,E}$ at total energy $E > 0$ above the ionization threshold energy of the $N_0 + 1$ electron system ($E = 0$).

$$\Psi^-_{\alpha,E} = \sum_n B_{\alpha,n}(E)\Psi_n{}^0 + \sum_\beta \int_0^\infty dE' C_{\alpha,\beta}(E,E')\Psi_{\beta,E'}{}^0. \tag{7a}$$

Those bound states which have eigenvalues $E_n \geq 0$ lie within the continuum and are of course referred to as resonance states.

It shall be understood that the wave functions $\Psi_n{}^0$ and $\Psi_{\beta,E'}{}^0$ and therefore $\Psi^-_{\alpha,E}$ have been separately diagonalized with respect to the total orbital angular momentum $\vec{J}$, total electron spin $\vec{S}$, and possibly with respect to other operators. These operators are assumed to commute with $H$ and with each other and produce quantum numbers which are "conserved" throughout the collision. Therefore all quantities are to be considered implicit functions of such quantum numbers.

### B. Boundary Conditions and Scattering Matrix

Asymptotically, as the electron coordinate $r$ approaches infinity, we require that the total wave function take the following, incoming wave form

$$\Psi^-_{\alpha,E} \rightarrow \sum_\gamma \mathcal{Y}_\gamma [-i/r(v_\gamma h)^{\frac{1}{2}}] \times [S_{\alpha,\gamma} e^{+ik_\gamma r - i\frac{1}{2}\pi l} - \delta_{\alpha,\gamma} e^{-ik_\gamma r + i\frac{1}{2}\pi l}], \tag{8a}$$

where $S$ is the scattering matrix. $\mathcal{Y}_\gamma$ are the total angular momentum states for a given $\vec{J}$ and $\vec{S}$, and are constructed from a linear combination of the asymptotic target states, M($s$), coupled to the electron spin $\sigma$ and orbital angular momentum states (or partial waves) $l$ of the free electron. Each $\mathcal{Y}_\gamma$ designates a separate, orthonormal "channel" $\gamma = (s,l)$. $W_S$ is the eigenvalue of the target in quantum state $s$, $v_\gamma$ is the velocity, $\epsilon$ is the kinetic energy and $k_\gamma$ is the wavenumber of the free electron. $E = W_S + \epsilon$ and the threshold for each channel $(s,l)$ occurs when $E = W_S$.

An alternate, standing wave, representation of the total wave function is

$$\Psi_{\alpha,E} \rightarrow \sum_\gamma \mathcal{Y}_\gamma [2/r(v_\gamma h)^{\frac{1}{2}}] \times U_{\alpha,\gamma} \sin(k_\gamma r - \tfrac{1}{2}\pi l + \eta_\alpha), \tag{8b}$$

where $U_{\alpha,\gamma}$ is a real, orthogonal matrix, $\tilde{U}\,U = 1$, which diagonlizes both the scattering matrix $S$ and the reactance matrix $K$. The $[\eta\alpha]$ are the eigen-phases, and together with $U$ define $S$ and $K$,

$$S = \tilde{U} e^{i2\eta} U - (1 + jK)(1 - iK)^{-1} \tag{9}$$

$$K = \tilde{U} \tan\eta\, U = i(1 - S)(1 + S)^{-1}. \tag{10}$$

It is useful to define a matrix $A = e^{i\eta}U$, such that

$$S = \tilde{A}A \tag{11}$$

and $$A^*\tilde{A} = \tilde{A}^*A = 1. \tag{12}$$

With these definitions it may be seen that the set of states $\{\Psi_{\alpha,E}\}$ are both real and orthonormal [in the sense of Eq. (5)] with a degeneracy corresponding to the number of open channels $\{\gamma\}$. The more usual incoming, $\{\Psi^-_{\alpha,E}\}$, or outgoing, $\{\Psi^+_{\alpha,E}\}$, representations[4] of the continua are complex, and are given by the following transformations of the standing wave representation $\{\Psi_{\alpha,E}\}$,

$$\Psi^+ = \tilde{A}^*\Psi, \tag{13a}$$

and $$\Psi^- = S\Psi^+ = \tilde{A}\Psi^+. \tag{13b}$$

By definition the resonance states $\Psi_n{}^0$ vanish as $r \rightarrow \infty$, while the approximate continuum functions $\Psi_{\beta,E}{}^0$ obey the boundary conditions (8) and define an approximate scattering matrix $S^0$ together with the matrices $U^0$, $e^{i2\eta^0}$, and $A^0$. We have employed

the standing wave representation $\Psi_{\beta,E}{}^{0}$ in Eq. (7a) merely for the convenience of having a real CI matrix $V$ in Eq. (6a). In the sense that the approximate scattering matrix $S^0$ may include off-diagonal terms the effect of inelastic potential scattering is introduced into our final solutions.

### C. General Solution

Using Eq. (7a) in the Schroedinger equation $(H-E)\Psi_{\bar{\alpha},E}=0$, and employing Eqs. (4), (5), and (6) we generate linear equations in the unknown matrices $B$ and $C$. These matrix equations may be solved following Fano's prescriptions. The critical step is to express $C$ in terms of a principal value and a delta function,

$$C_{\alpha,\beta}(E,E') = \mathcal{P}[Y_{\alpha,\beta}(E,E')/E-E'] + Z_{\alpha,\beta}(E)\delta(E-E') \ , \tag{14}$$

where $\mathcal{P}$ indicates that the principal value should be taken. Then in matrix form we find[5]

$$Y' = BV' \tag{15}$$

and $$B(E1-F) = Z\tilde{V} \tag{16}$$

where 1 is the unit matrix and $F$ is a symmetric real matrix,

$$F_{n,m}(E) = E_n\delta_{n,m} + \mathcal{P}\int_0^\infty dE' \times \sum_\beta V_{n,\beta}(E,E')V_{m,\beta}(E,E')/(E-E') \tag{17}$$

The net effect of the integrals in Eq. (17) is to introduce couplings between the zero-order resonance states due to their mutual interactions with the continua and to produce apparent shifts in the locations of the resonance states. It proves convenient to define a new set of shifted resonance states $\{\Psi_n{}^{\text{shift}}\}$ which are diagonal with respect to these interactions. The "locations" $\mathcal{E}_n$ of the transformed states are given by the eigenvalues of $F$

$$F = \tilde{G}\mathcal{E}G \tag{18}$$

where $\mathcal{E}=\mathcal{E}_n\delta_{n,m}$ and $G$ is real and orthogonal $\tilde{G}G=1$, and defines the transformation

$$\Psi_n{}^{\text{shift}} = \sum_m G_{n,m}\Psi_m{}^0 \tag{19}$$

We may regroup Eq. (7a) to form an alternative representation of the total wave function in terms of this set

$$\Psi_{\alpha,E} = \sum_n \mathcal{B}_{\alpha,n}\Psi_n{}^{\text{shift}} + \sum_\beta \int_0^\infty dE' C_{\alpha,\beta}(E,E')\Psi^0_{\beta,E'} \tag{7b}$$

Where $\mathcal{B}=B\tilde{G}$. Henceforth we will refer to $\{\Psi_n{}^{\text{shift}}\}$ as our set of resonance states and view the resonance energies $\mathcal{E}_n$ and new CI matrix $\mathcal{V}'$,

$$\mathcal{V}_{n,\beta}(E,E') = \langle \Psi_n{}^{\text{shift}}|H-E|\Psi_{\beta,E'}{}^{0}\rangle = \sum_m G_{n,m}V'_{m,\beta} \tag{6b}$$

as the fundamental microscopic properties which are to be extracted from an analysis of experimental data, rather than $E_n$ and $V'_{n,\beta}$. In principle these two sets of quantities are related through Eqs. (17), (18), and (19).

From Eqs. (16) and (17) we find that both $\mathcal{B}$ and $Y'$ are proportional to $Z$

$$\mathcal{B} = Z\tilde{\mathcal{V}}(E-\mathcal{E})^{-1}, \tag{20}$$

$$\pi Y' = Z\mathcal{K}', \tag{21}$$

where $$\mathcal{K}' = \pi\tilde{\mathcal{V}}(E-\mathcal{E})^{-1}\mathcal{V}'. \tag{22}$$

We are left with the one unknown matrix, $Z$, which we determine by imposing the asymptotic conditions in Eq. (8a) on Eq. (7b). We substitute Eq. (14) for $C$ and express $\Psi_{\alpha,E'}{}^{0}$ in terms of its asymptotic form Eq. (8b) with its associated matrices $U^0$ and $A^0$. Noting that

$$\mathcal{P}\int dE' \frac{e^{\pm ikr}}{E-E'} \xrightarrow[r\to\infty]{} \pm i\pi e^{+ikr}$$

we obtain the following matrix equations from Eq. (8a),

$$1 = Z(I+i\mathcal{K})A^{0*}, \tag{23}$$

$$S = Z(I-i\mathcal{K})A^0. \tag{24}$$

From Eq. (23) we obtain the following expression for $Z$[6]

$$Z = \tilde{A}^0(1+i\mathcal{K})^{-1}. \tag{25}$$

We now have a complete orthonormal solution for the total wave function Eq. (7b) in terms of Eqs. (14), (20)–(23). It is useful to follow Fano's lead and define a "modified resonance state" which includes an admixture of continuum states,

$$\Phi_n{}^0 = \Psi_n{}^{\text{shift}} + \sum_\beta \mathcal{P}\int_0^\infty dE' \frac{\mathcal{V}'_{n,\beta}\Psi_{\beta,E'}}{E-E'} \ . \tag{26}$$

Then the total wave function takes the following pleasing form,

$$\Psi^-_{\alpha,E} = \sum_\beta Z_{\alpha,\beta}\{\Psi_{\beta,E}{}^0 + \sum_n \frac{\mathcal{V}_{n,\beta}}{E-\mathcal{E}_n}\Phi_n{}^0\} \tag{27}$$

The basic problem in employing this generalized CI theory will be to construct $\mathcal{K}$ in Eq. (22) and to invert $(1+i\mathcal{K})$ in order to obtain the normalization matrix $Z$ in Eq. (25). The scattering matrix Eq. (24) is also given in terms of this inversion

$$S = \tilde{A}^0\mathcal{S}A^0 \tag{28}$$

where

$$\mathcal{S} = (1+i\mathcal{K})^{-1}(1-i\mathcal{K}). \tag{29}$$

It is apparent from Eq. (9) that $\mathcal{K}$ is closely related to the reactance matrix $K$ and incorporates the

effect of the resonance states on the scattering matrix.

For a description of resonant electron scattering, i.e., Eq. (1), the expression for the $S$ matrix is all we require. However, to obtain the photoionization cross sections, i.e., Eq. (2), we now must introduce the expression for the total wave function Eq. (27) into Eq. (3).

### D. Photo-ionization

The total cross section for photoionization from the initial bound state $\Psi_i$ into the continuum channel $\alpha$ is given by Eq. (3),

$$\sigma_{\alpha,E} = |t^-_\alpha|^2, \tag{30}$$

where $t^-_\alpha$ is the element of the coluum vector $t^-$ of transition amplitudes[7] for the total incoming wave functions $\Psi^-_{\alpha,E}$,

$$\{t^-_\alpha\} = \langle \Psi^-_{\alpha,E} | T | \Psi_i \rangle \tag{31}$$

The total photoionization cross section into all channels is then

$$\sigma_E = \tilde{t}^{-*} t^- \tag{32}$$

We define similar column vectors for the "resonance" states $\Phi_n{}^0$ and the continuum states $\Psi_{\beta,E}{}^0$ in Eq. (27).

$$\{t_n{}^b\} = \langle \Phi_n{}^0 | T | \Psi_i \rangle, \tag{33}$$

$$\{t_\alpha{}^c\} = \langle \Psi_{\beta,E}{}^0 | T | \Psi_i \rangle \tag{34}$$

and obtain the following matrix equation for $t^-$

$$t^- = Z\{t^c + \mathcal{V}(E-\mathcal{E})^{-1} t^b\}. \tag{35}$$

In terms of the present notation, Fano's $q_n$ and $\rho_n$ factors[8] for each resonance state $\Phi_n{}^0$ are defined as follows

$$q_n = t_n{}^b / \pi \textstyle\sum_\beta \mathcal{V}_{n,\beta}\, t_\beta{}^c, \tag{36}$$

$$\rho_n = \frac{\sum_\beta \mathcal{V}_{n,\beta} t_\beta{}^c}{\left(\sum_\beta \mathcal{V}^2_{n,\beta}\right)^{\frac{1}{2}} \left[\sum_\beta (t_\beta{}^c)^2\right]^{\frac{1}{2}}} \tag{37}$$

Equation (35) can be expressed as follows

$$t^- = Z\left(1 + \tilde{\mathcal{V}}\left(\frac{\pi q}{E-\mathcal{E}}\right)\mathcal{V} t^c\right) \tag{38}$$

where $\pi q/(E-\mathcal{E})$ is a diagonal matrix, $(\pi q_n/(E-\mathcal{E}_n)]\delta_{n,m}$.

### E. Widths and Overlap Matrix

The partial width which represents the coupling of the resonance $\Psi_n{}^{\text{shift}}$ to the standing wave continuum $\Psi_{\beta,E}{}^0$ is given by the CI matrix $\mathcal{V}$,

$$\Gamma_{n,\beta} = 2\pi \mathcal{V}^*_{n,\beta} \mathcal{V}_{n,\beta} \tag{39}$$

The total width $\Gamma_n$ is the sum over all channels $\beta$

$$\Gamma_n = \textstyle\sum_\beta \Gamma_{n,\beta} = 2\pi \sum_\beta \mathcal{V}^*_{n,\beta} \mathcal{V}_{n,\beta}. \tag{40}$$

These widths are implicit functions of $E$. It is usually assumed that any variation with $E$ is small over the range of energies $E \approx \mathcal{E}_n \pm \Gamma_n$ and that $\Gamma_n(E) \approx \Gamma_n(E_n)$. This assumption will be employed throughout the remainder of this paper.

For each resonance $\Psi_n{}^{\text{shift}}$ there is a linear combination of continua which embodies the total CI between $n$ and the set of $\Omega$ open channels $\{\beta\}$,[8]

$$\Psi^{(n)}_{\alpha=1,E} = (2\pi/\Gamma_n)^{\frac{1}{2}} \textstyle\sum_\beta \mathcal{V}_{n,\beta} \Psi_{\beta,E}{}^0. \tag{41}$$

There are $(\Omega-1)$ remaining continua $(\alpha = 2,\Omega)$ which are orthonormal to $\Psi^{(n)}_{1,E}$ *and* orthogonal to $\Psi_n{}^{\text{shift}}$ and represent the background scattering. [These transformed continua are employed in the definitions[8] of $q_n$ and $\rho_n{}^2$ in Eqs. (36) and (37)]. If the various continua $\Psi^{(n)}_{1,\alpha}$ for each $(n)$ are mutually orthogonal there is no interaction between the resonances due to CI with the continua and each may be treated as a single, isolated resonance imbedded in its own continuum. However, as is more likely, these continua will not be orthogonal, and the complications due to overlapping, or interference between neighboring resonances, is introduced.

We define an "overlap matrix" between the continua as follows,

$$\mathcal{O}_{n,m}\delta(E-E') = \langle \Psi^{(n)}_{1,E} | \Psi^{(m)}_{1,E'} \rangle \tag{42}$$

or

$$\mathcal{O}_{n,m} = [(2\pi)^2/\Gamma_n\Gamma_m]^{\frac{1}{2}} \textstyle\sum_\beta \mathcal{V}^*_{n,\beta} \mathcal{V}_{m,\beta}. \tag{43}$$

If $\mathcal{O}=1$ then we say the resonances are *superimposed* and they may be treated as isolated, while $\mathcal{O} \neq 1$ implies nonvanishing off-diagonal terms and indicates *overlapped* resonances.

It is our purpose to emphasize the general consequence of overlapping, $\mathcal{O} \neq 1$, and several models of atomic and molecular systems are constructed to demonstrate these effects. But first we will discuss the general theory and compare it with previous results.

## III. DISCUSSION

### A. General Features

The basic problem in analyzing resonance phenomena is to extract information about the resonance states, primarily from the energy dependence of the scattering or photoionization cross sections. This energy dependence is ultimately related to the energy dependence on the energy shell $E' = E$ of the $\Omega \times \Omega$ reactance matrix $\mathcal{K}(E)$ in Eq. (22), where $\Omega$ is the number of open channels $\{\alpha\}$,

$$\mathcal{K}_{\alpha,\beta}(E) = \sum_{n=1}^{N} \frac{\pi \mathcal{V}_{n,\alpha} \mathcal{V}_{n,\beta}}{E - \mathcal{E}_n} \tag{44}$$

Each resonance system is defined by the $N\times\Omega$ CI matrix $\mathcal{U}$, where $N$ is the number of resonances $\Psi_n^{\text{shift}}$, and by the location of the resonances $\mathcal{E}_n$. To obtain explicit expressions for the cross section our major problem is to invert $(1+i\mathcal{K})$, or to diagonalize the real, symmetric matrix $\mathcal{K}$,

$$\mathcal{K} = -\tilde{\mathcal{U}} \tan \mathcal{U} \tag{45}$$

where $\mathcal{U}$ is orthogonal and -tan $\delta$ are the eigenvalues of $\mathcal{K}$.

The fundamental quantities we wish to extract from an analysis of resonance phenomena are the resonance energies $E_n$, and the CI matrix $V'_{n,\alpha}$ in Eq. (6a), and actually Eq. (44) can be made an explicit function of these quantities, i.e., $\mathcal{K}=\tilde{V}(E-F)^{-1}V$. However, if $V$ and $\mathcal{U}$ are slowly varying functions of $E$, then Eq. (44) is in the form which exhibits the most explicit, and irreducible representation of the $E$ dependence of $\mathcal{K}$. Thus the only quantities we can hope to extract from an analysis of the cross sections are the resonance energies $\mathcal{E}_n$, and CI matrix $\mathcal{U}$ for the *shifted* resonance states $\Psi_n^{\text{shift}}$, and we must view these as our fundamental microscopic properties. To go any further in the analysis requires an *a priori* knowledge of the shift matrix $G$ defined by Eq. (18). However, we should be aware that because of the mixing of the zero-order states $\Psi_n^0$ in Eq. (19) simplifying assumptions which are often applied to $\Psi_n^0$, such as factoring out a Rydberg series like dependence on the principal quantum number, might not be at all valid for $\Psi_n^{\text{shift}}$. As will become evident in the discussion, and model calculations which follow, we shall in fact apply various simplifying models directly to $\Psi_n^{\text{shift}}$ and make no further reference to the shift matrix $G$. Our main purpose in the model calculations is to demonstrate the effects which can occur when resonances overlap. The further complications introduced by $G$ merely reinforce our contention that the parameters one extracts from situations involving overlapping are often far removed and only indirectly related to the unperturbed resonance states $\Psi_n^0$, or $\Psi_n^{\text{shift}}$.

For purposes of demonstration we will construct two model systems which might reasonably represent the effects of overlapping resonances. One is a model for the photoionization of atoms in the far uv and the other is a model for electron-diatomic molecule scattering. But first let us demonstrate the agreement of the present results with previously derived special cases and demonstrate some overlapping effects.

### B. Comparison With Previous Results

The cases treated previously[1,8] correspond to special cases of the following assumption,

$$\mathcal{U}_{n,\alpha} = v_n f_\alpha \tag{46}$$

where $\sum_\alpha f_\alpha{}^2 = 1$. This is equivalent to assuming that all resonances have identical branching ratios into the set of open channels, i.e., $\Gamma_{n,\alpha} = f_\alpha{}^2\Gamma_n$, and ,

$$\Gamma_n = 2\pi v_n{}^2 \tag{47}$$

In view of Eq. (41) assumption Eq. (46) merely states that all resonances interact with just one continuum

$$\Psi_{1,E}^{(\text{all})} = \sum_\beta f_\beta \Psi_{\beta,E}{}^0$$

and we have simply reduced to Fano's many-resonance one continuum case.[1] The eigenvalues of $\mathcal{K}$ [see Eq. (45)] are

$$-\tan\delta_\beta = \delta_{1,\beta} \sum_n \tfrac{1}{2}\Gamma_n/(E-\mathcal{E}_n)$$

and the eigenvector for $\beta = 1$ is

$$\mathcal{U}_{1,\gamma} = f_\gamma .$$

We need not know the other $\Omega-1$ vectors, $\beta>1$, other than that they are orthogonal to $\mathcal{U}_{1,\gamma}$. The resultant $\mathcal{S}$ matrix (Eq. 29) is[9]

$$\mathcal{S}_{\alpha,\beta} = \delta_{\alpha,\beta} - 2if_\alpha f_\beta g/(1+ig) \quad , \tag{48}$$

where $g = \sum_n \Gamma_n/2(E-\mathcal{E}_n)$ . (49)

For this special case the photoabsorption cross section is, from Eqs. (32) and (38)

$$\sigma = \sigma_b + \sigma_a \frac{[1+\sum_n \tfrac{1}{2}\Gamma_n q_n/(E-\mathcal{E}_n)]^2}{(1+g^2)} \tag{50}$$

where $\sigma_b = \tilde{t}^c t^c - \sigma_a$, $\sigma_a = (\tilde{f}\,t^c)^2$, and $q_n = t_b{}^n/\pi \tilde{f} t^c$, in agreement with Ref. 1. In this case all resonances couple to one continuum and the overlap Eq. (43) is a maximum, i.e., $\Theta_{n,m}=1$ for all $n$ and $m$.[10,11] This effect was discussed briefly by Fano.[1] Notice that if all $q_n$ have the same sign the second term in Eq. (50) must pass through zero, i.e.,

$$1+\sum_n \tfrac{1}{2}\Gamma_n q_n/(E-\mathcal{E}_n) = 0,$$

once between each resonance $\mathcal{E}_n$, $\mathcal{E}_{n+1}$, regardless of the widths $\Gamma_n$. Thus, if $\sigma$ is interpreted as a superposition of isolated resonances the "apparent" widths of the resonances would never exceed the spacings. In fact if the widths become exceedingly large, i.e., $\Gamma_n \gg E_n - E_{n-1}$ the cross section Eq. (50) takes on the appearance of a series of narrow isolated resonances. Consider the case of $q_n = Q =$ constant for all $n$. Then

$$\sigma = \sigma_b + \sigma_a(1+Qg)^2/(1+g^2).$$

In the limit, as $\langle\Gamma_n\rangle_{\text{av}} \gg \langle\mathcal{E}_{n+1}-\mathcal{E}_n\rangle_{\text{av}}$, the cross section can be represented as a superposition of narrow resonances.

$$\sigma \xrightarrow[\Gamma\to\infty]{} \sigma_b + \sum_m \sigma_a Q^2(\epsilon_m - Q^{-1})^2/(1+\epsilon_m{}^2),$$

where $\epsilon_m = 2(E-D_m)/\tilde{\Gamma}_m$. The "shifted" resonance energies $D_m$ are located at the singularities

of $f = -1/g$ and thus are the roots of $g(E) = 0$. It can be shown that the reciprocal of $-g$ must take the following form.[12]

$$f = \alpha E + \beta + \sum_m \tilde{\Gamma}_m / 2(E - D_m),$$

where the "widths" are

$$\tilde{\Gamma}_m = \left[\sum_n \Gamma_n / 2(\epsilon_n - D_m)^2\right]^{-1}$$

In the limit, as $\Gamma \to \infty$, $\alpha$, $\beta \to 0$ for finite $E$, and we obtain the limiting case shown above.

This narrowing effect is shown in Fig. 1 for a Rydberg series of resonances. Notice how the location and "apparent" widths change as $\Gamma_n$ is increased, until we attain what appears to be narrow, isolated resonances in the limit of large $\Gamma_n$.

## IV. ATOMIC RYDBERG SERIES OF AUTOIONIZING LINES

In what follows we assume that for a given series $\lambda$ the resonance energies (in rydbergs) are spaced as follows,[8]

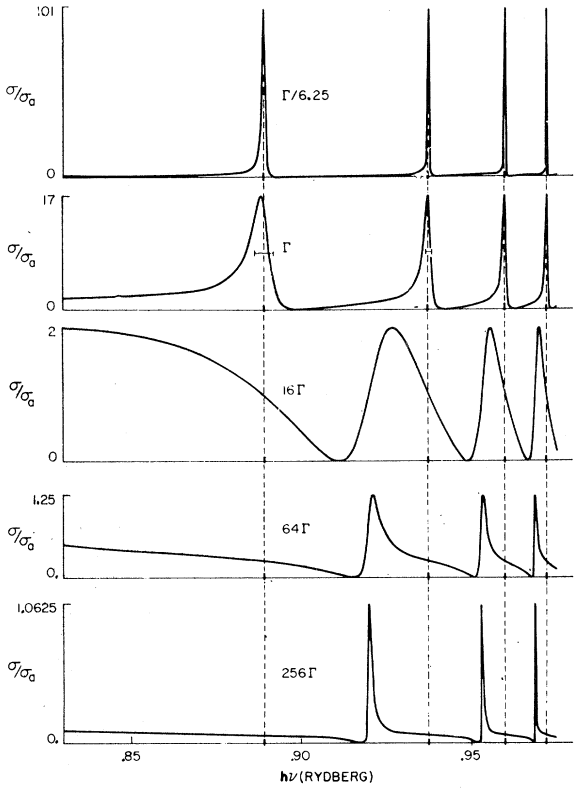


FIG. 1. Photoabsorption cross section for an autoionizing series of Rydberg lines, as a function of increasing width. The transition amplitudes to the Rydberg states and to the continuum are held constant so the magnitude of the $q$ factor does vary as $\Gamma$ increases. Note that in the limit of very large overlapping widths the cross section takes on the appearance of a single series of narrow resonances located at intermediate distances between the original resonances (located by the ticks).

$$\mathcal{E}_n = \mathcal{E}_{\lambda,p} = \mathcal{E}_\lambda - (p - p_\lambda^*)^{-2}. \tag{51}$$

$p$ is the principal quantum number, and $p^*$ is the quantum defect. The transition amplitudes $t_n{}^b$ are approximated as follows,

$$t_{\lambda,p}{}^b = t_\lambda{}^b R_{\lambda,p} \tag{52}$$

where[13]

$$R_{\lambda,p}{}^2 = 2(p - p^*_\lambda)/[(p - p^*_\lambda)^2 - 1]^2 \tag{53}$$

We will distinguish between two types of ionization processes. We call the first "autoionization" and its partial widths "autoionization widths"; in this case the CI matrix Eq. (6b) is proportional to $R_{\lambda,p}$,

$$v_{n,\beta} = v_{\lambda,\beta}{}^{\text{auto}} R_{\lambda,p} \tag{54}$$

The reasons for this dependence have been discussed elsewhere.[8] Note that within a given series $\lambda$ each resonant state $p$ autoionizes to identically the same continuum Eq. (41) and the overlap Eq. (43) between all resonances in the series is one.

In the second process we refer to Auger widths. The resonances are due to excitation of inner shell electrons. The core may undergo an Auger ionization in which the Rydberg electron does not participate. In this case the CI matrix elements are equal for all members of the series $p$.

$$v_{n,\beta} = v_{\lambda,\beta(p)}{}^{\text{Auger}} \tag{55}$$

However there is another important distinction in this case; each resonance ionizes into a separate continuum $\beta = \beta(p)$, leaving the ion in the excited Rydberg state $p$, and the overlap between resonances is zero. The transition amplitudes into the Auger continua should vary approximately as $t_{\beta(p)}{}^c = t_\lambda{}^{\text{Auger}} R_{\lambda,p}$.[8]

### A. Overlapping Autoionizing Series

Figure 1 already demonstrates the effect of increasing the widths on the photoabsorption for a single "autoionizing" Rydberg series. However we often expect the occurrence of several closely lying Rydberg series which can couple to common continua. As a trivial application of the present theory let us vary the degree of overlap between two autoionizing series $\lambda = 1,2$ which have only a small difference in their quantum defects, e.g., $p_1^* - p_2^* = 0.1$. The other variables are the total widths $\Gamma_n$ Eqs. [(40), (53), (54)], a constant $q$ factor Eq. (36), and a constant $\rho^2$ factor Eq. (37) for each series. These parameters are kept constant; $\rho^2 = 0.5$ for both series and $q = 2\sqrt{2}, -2\sqrt{2}$ for series 1 and 2, respectively. Figure 2 shows the effect of increasing the overlap between the series on the total photoabsorption cross section. Of course within each series $\lambda$ the overlap between all $p$ states is one, just as in Fig. 1. Notice that in all three curves the total widths (shown by bars in Fig. 2A) $\rho^2$, and $q$ are the same. *The only variable is the degree of overlap between the series,* And yet, as seen in Figs. 2B, and 2C, with

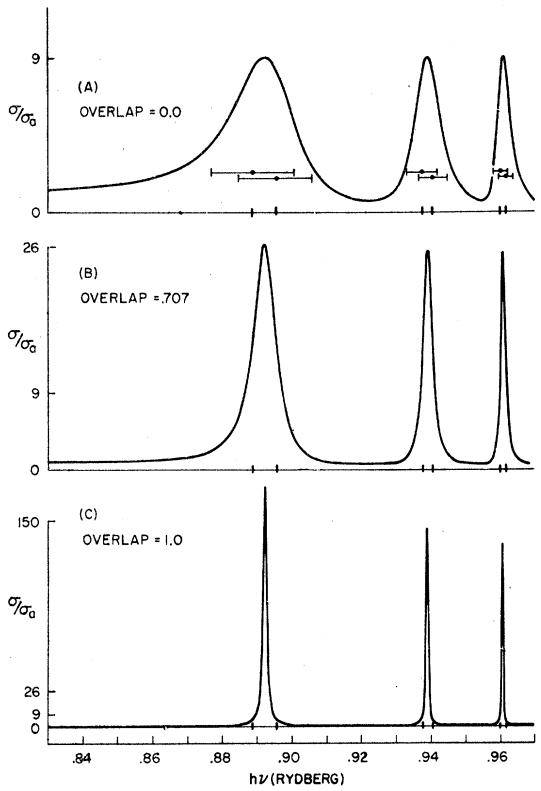


FIG. 2. Overlapping between two closely lying Rydberg series. Series 1, located by the first of each pair of ticks, has $\rho^2 = 0.5$ and a constant $q$ factor of $8^{1/2}$. The second series has a $\rho^2 = 0.5$ and a $q = -8^{1/2}$. The cross sections are normalized to the total continuum cross section, i.e., $\sigma a \equiv \tilde{t}_c t_c$. The total widths are the same in all three plots and are shown by the bars in (A). *The only difference between the plots is the degree of overlap.* (A) The overlap is zero between the two series, i.e., they autoionize to orthogonal continua, and their photoabsorption cross sections merely superimpose. (B) Here the degree of overlap is 0.707. (C) In this extreme case both series autoionize to the same continua and this causes the oscillator strength to accumulate in the narrow region between the two series in spite of the fact that the widths are the same as in (A) and (B).

increasing overlap the oscillator strength has "collected" in the narrow interval between adjacent resonances, and the "apparent" width bears no resemblance to actual widths which are shown in Fig. 2A. When the overlap equals 1 as in Fig. 2C the cross section is given by Eq. (50). Because of the difference in the sign of $q$ the sum $(1 + \frac{1}{2}\Sigma q_n \Gamma_n / E - \varepsilon_n)$ in Eq. (50) has alternating signs and the $\sigma_a$ term does not necessarily vanish between resonances; actually the cross terms add in the narrow interval between resonances.

In Fig. 3 we show a similar case, where $q = +2\sqrt{2}$ for both series. The sum now must vanish between all resonances, and the oscillator strength is spread out, while the cross section exhibits a "window" in the narrow intervals.

It is apparent from this exercise that without prior knowledge of the overlap matrix $\mathcal{O}$ it is an impossible task to extract meaningful values of $\Gamma$, $q$, and $\rho^2$ for such series.

### B. Overlapping Auger Widths

It is a trivial matter to treat the Auger mechanism alone since each resonance has a constant width and does not overlap with its neighbors, i.e., $\mathcal{O}_{n,m} = 0$ for $n \neq m$, and the spectra is just a superposition of isolated resonances. However, we might expect that the same resonance states will also "auto-ionize". The mixed case, with partial widths for both processes, can only be handled by the present theory.

For a single Rydberg series of $N$ resonances there are $N+1$ channels, i.e., $\Omega = N+1$ in Eq. (44).[14] An example of the resultant total cross section for such a situation is shown in Fig. 4A.[15] Notice how the resonance peak heights decrease in amplitude in contrast to the pure autoionization processes. The interesting features for this case are the photo-ionization cross sections into the individual channels. Figure 4B shows the auto-ionization cross section, while Figs. 4C and 4D show the cross sections into the Auger channels associated with the first and second resonances. The

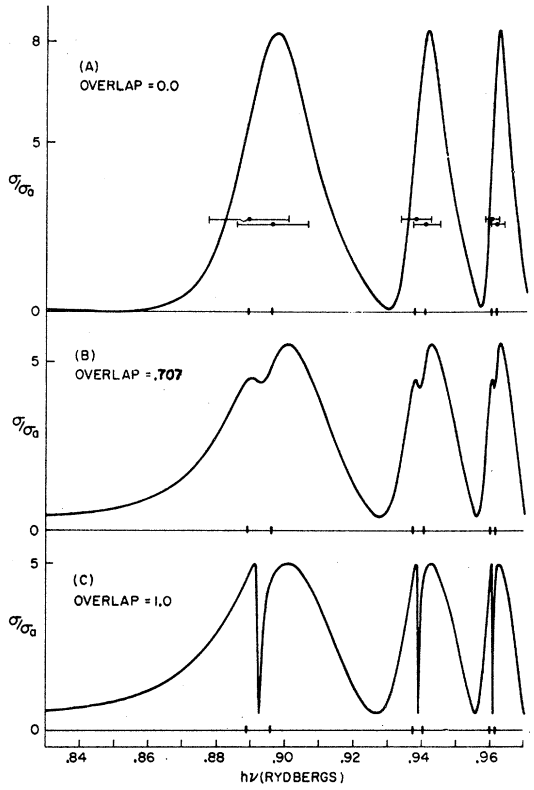


FIG. 3. Overlapping between two closely lying Rydberg series. Same as Fig. 2 except both series have a positive $q = 8^{1/2}$. In this case the oscillator strength is spread out and a "window" develops between the resonance as the degree of overlap increases.

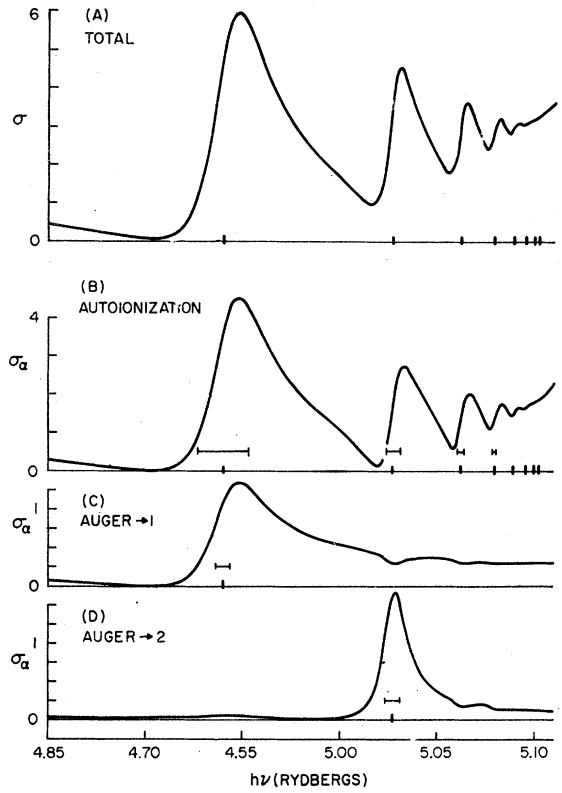


FIG. 4. Effect of combined autoionization and Auger processes on a single Rydberg series. The partial "autoionization widths" are shown by the bars in (B), while the "Auger widths" which are constant for each resonance are shown by the bars in (C) and (D). All resonances have a constant $q = 1.98$, while $\rho^2$ decreases with increasing principal quantum number $p$; the first few values are 0.90, 0.58, 0.35, 0.21. Also the degree of overlap decreases rapidly with increasing $p$; $\Theta_{1,2} = 0.623$; $\Theta_{1,3} = 0.439$; $\Theta_{2,3} = 0.352$. All the cross sections are normalized to unit cross section for photoabsorption into the autoionization continuum. (A) shows the total photoabsorption. (B) is the partial cross section into the autoionization channel to which all the resonances are coupled. (C) is the cross section for photoionization into the Auger channel which leaves the ion in the excited Rydberg state corresponding to the first resonance. (D) is the partial cross section into the Auger channel arising from the second resonance.

partial widths for the various channels are indicated by bars in Figs. 4B–4D. Notice that, because of the off-diagonal couplings in $\mathcal{K}$, the Auger channels show a slight structure due to neighboring resonances which would be absent in the pure Auger case. Supposedly one could observe these partial cross sections by energy analyzing the photoelectrons. Each channel would give rise to a different ejected electron energy. However this effect is not very striking, particularly once the Auger widths equal or exceed the autoionization widths. But again it does reflect the ambiguities which might arise if overlapping effects are not considered. On the basis of the total cross section alone it would be impossible to estimate the degree of overlap. The partial cross sections often can offer the added information needed to properly interpret the spectra.

## V. OVERLAPPING RESONANCES IN ELECTRON-MOLECULE SCATTERING

We construct a rather special molecular model which, however, demonstrates the effects introduced by the overlap of resonances coupled to the same channels. Consider an electron incident on $H_2$ in its ground electronic state and in vibrational state $\alpha = 0$. This is represented in Fig. 5. Each vibrational state $\alpha$ corresponds to an open channel

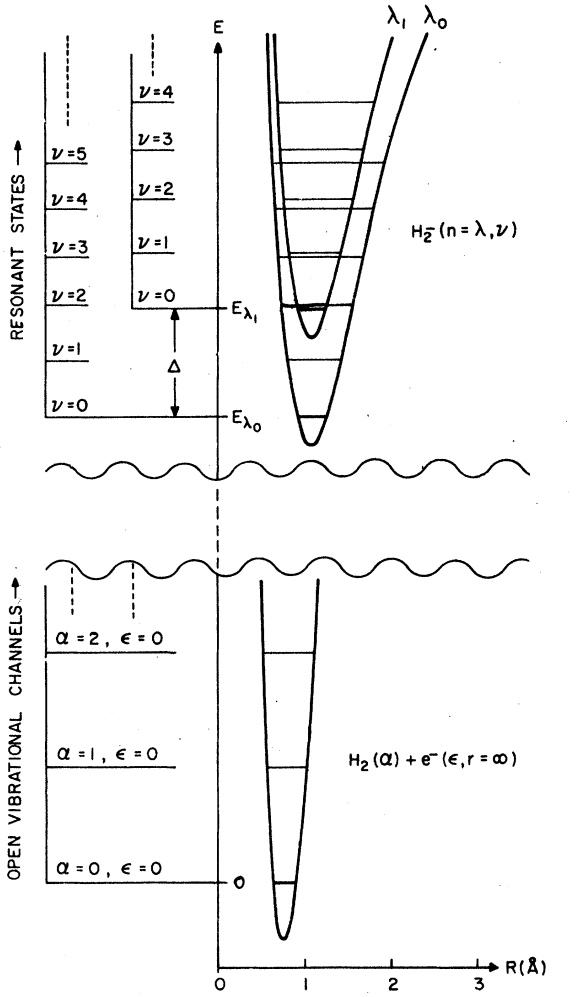


FIG. 5. Model of electron-molecule scattering using $H_2$ potentials. Each vibration state $\alpha$ of the ground electronic state corresponds to an open channel. Two electronic resonances are postulated, $\lambda_1$ and $\lambda_2$, both of which are represented by the $H_2^+$ potential, and have identical vibrational spectra. The spacing between the onset of the two series, $\Delta$, is taken to be 1.86 times the vibrational quanta $\hbar\omega_e$. This model is not to be taken as a meaningful representation of the real $H_2$ system, but was merely devised to demonstrate overlapping effects.

and $\epsilon$ is the asymptotic kinetic energy of the electron. We assume several electronic resonance states exist, which arise from doubly excited states of $H_2^-$. In order to simplify the problem we assume each electronic state $\lambda$ has identically the same potential curve and hence vibrational wave functions $\varphi$. In the model calculations we consider the overlap of the two states $\lambda_0$ and $\lambda_1$ shown in Fig. (5). These are approximated by the $H_2^+$ potential. In addition we assume that the only open channels are the vibrational states $\alpha$; in terms of electronic states alone we might say we are treating the case of one open electronic channel coupled to several electronic resonances. *This model is constructed strictly for demonstration purposes and is not meant to describe the actual electron-$H_2$ scattering.*

We employ the adiabatic Born approximation and factor the zero-order functions into a product of vibrational functions times electronic-rotational functions.

$$\Psi_n^{\text{shift}} = \Psi_\lambda^{\text{el}} \varphi_\nu(R), \quad n = (\lambda, \nu) \tag{56}$$

with $\mathcal{E}_n = E_\lambda + E_\nu$,

and $$\Psi_{\alpha, E}^{0} = \Psi_\epsilon^{\text{el}} \xi_\alpha(R) \tag{57}$$

with $E = \epsilon + E_\alpha$.

We can define an electronic CI integral

$$\mathcal{V}_\lambda(R) = \langle \Psi_\lambda^{\text{el}} | H - E | \Psi_\epsilon^{\text{el}} \rangle \tag{58}$$

and also an $R$ dependent "electronic width"

$$\Gamma_\lambda(R) = 2\pi \mathcal{V}_\lambda^2. \tag{59}$$

If the dependence of Eq. (58) on the vibrational coordinate $R$ can be ignored then Eq. (6b) can be factored into an electronic term times a vibrational overlap integral between the channel vibrational states $\xi_\alpha$ and the resonance vibrational states $\varphi_\nu$.

$$\mathcal{V}_{n,\alpha} = \langle \varphi_\nu | \mathcal{V}_\lambda(R) | \xi_\alpha \rangle \approx \mathcal{V}_\lambda F_{\nu,\alpha} \tag{60}$$

where $$F_{\nu,\alpha} = \langle \varphi_\nu | \xi_\alpha \rangle . \tag{61}$$

Eq. (62) states that the partial width between the electronic-vibrational state $n$ and the open channel $\alpha$ is factored into an electronic width times a Franck-Condon factor $F_{\nu,\alpha}^2$.

$$\Gamma_{n,\alpha} \approx 2\pi \mathcal{V}^2{}_\lambda F_{\nu,\alpha}{}^2 = \Gamma_\lambda F_{\nu,\alpha}{}^2. \tag{62}$$

Since $F_{\nu,\alpha}$ is an orthogonal matrix the total width for the electronic-vibrational state $n$ is equal to $\sum \Gamma_{n,\alpha} = \Gamma_\lambda$, and each vibrational resonance state has the same width. This is only true if the *entire* set of vibrational channels are open. We assume the electronic resonance occurs at energies high enough above threshold that this is essentially true.

The overlap matrix for this case is

$$\mathcal{O}_{n,n'} = \sum_\alpha \mathcal{V}_\lambda \mathcal{V}_{\lambda'} F_{\nu,\alpha} F_{\nu',\alpha} = \mathcal{V}_\lambda \mathcal{V}_{\lambda'} \delta_{\nu,\nu'}. \tag{63}$$

Within a given electronic state the vibrational resonances are superimposed and do not overlap. This is strictly a consequence of assumption in Eq. (60) that the $R$ dependence of $\mathcal{V}_\lambda$ can be ignored.

It is a trivial matter to invert $(1 + i\mathcal{K})$ for this model. From Eqs. (44) and (60)

$$(1 + i\mathcal{K})_{\alpha,\beta} = \sum_\nu F_{\nu,\alpha} F_{\nu,\beta} (1 + i g_\nu), \tag{64}$$

where $$g_\nu = \sum_\lambda \Gamma_\lambda / 2(E - \mathcal{E}_{\lambda,\nu}). \tag{65}$$

Multiplying Eq. (64) from the right by $(1 + i\mathcal{K})^{-1}$ and from the left by $\tilde{F}(1 + ig)^{-1}F$, and making use of the identity $1 = F\tilde{F} = \tilde{F}F$, we obtain,

$$(1 + i\mathcal{K})^{-1}_{\alpha,\beta} = \sum_\nu F_{\nu,\alpha} F_{\nu,\beta} (1 + i g_\nu)^{-1}. \tag{66}$$

Then from Eq. (29) we find the $\mathcal{S}$ matrix

$$\mathcal{S}_{\alpha,\beta} = \sum_{\nu,\nu',\gamma} F_{\nu,\alpha} F_{\nu,\gamma} F_{\nu',\gamma} F_{\nu',\beta} \frac{1 - i g_{\nu'}}{1 + i g_\nu} . \tag{67}$$

If, and only if, the set of open channels $\{\gamma\}$ form a complete set, as we have assumed for the model in Fig. 5, then $\sum_\gamma F_{\nu,\gamma} F_{\nu',\gamma} = \delta_{\nu,\nu'}$ and Eq. (67) reduces to the following,

$$\mathcal{S}_{\alpha,\beta} = \sum_\nu F_{\nu,\alpha} F_{\nu,\beta} \frac{1 - i g_\nu}{1 + i g_\nu} . \tag{68}$$

We first consider the case of just one electronic resonance, i.e., $g_\nu = \frac{1}{2}\Gamma_{\lambda_0} / (E - \mathcal{E}_{\lambda,\nu})$. Equation (68) reduces to identically the same expression used by Chen in his analysis of the $N_2 + e$ resonances.[16]

$$\mathcal{S}_{\alpha,\beta} = \delta_{\alpha,\beta} - i \sum_\nu F_{\alpha,\nu} F_{\beta,\nu} \frac{\Gamma_{\lambda^0}}{E - \mathcal{E}_{\lambda,\nu} + i\Gamma_{\lambda_0}/2} . \tag{69}$$

This is just a superposition of *isolated* resonances, as indicated by Eq. (63). Figure 6 shows $1 - \text{Real}(\mathcal{S}_{0,0})$ for the $H_2$ model when one electron resonance $\lambda_0$ is present. If $A^0 = \hat{1}$ in Eq. (28) this is proportional to the total cross section. The widths are shown as bars and the curves are labeled according to $\Gamma_{\lambda_0}$ in units of the $0 - 1$ vibrational spacing $\hbar\omega_e$. The locations of the vibrational resonance states are shown at the bottom of the figure. As the width increases the curve exhibits a blending into a Franck-Condon "envelop". Similar behavior is seen in Fig. 7 for the $0 - 1$ vibrational excitation cross section. This is a consequence of having constructed $\mathcal{V}_{n,\alpha}$ in such a way that $\mathcal{S}$ and $\mathcal{K}$ are diagonalized by the matrix $F$. If the electronic widths are $R$ dependent this is no longer true and structure probably would persist even at large widths. But the overlapping effect is more easily demonstrated by allowing two electronic resonances $\lambda_0$ and $\lambda_1$ to overlap.

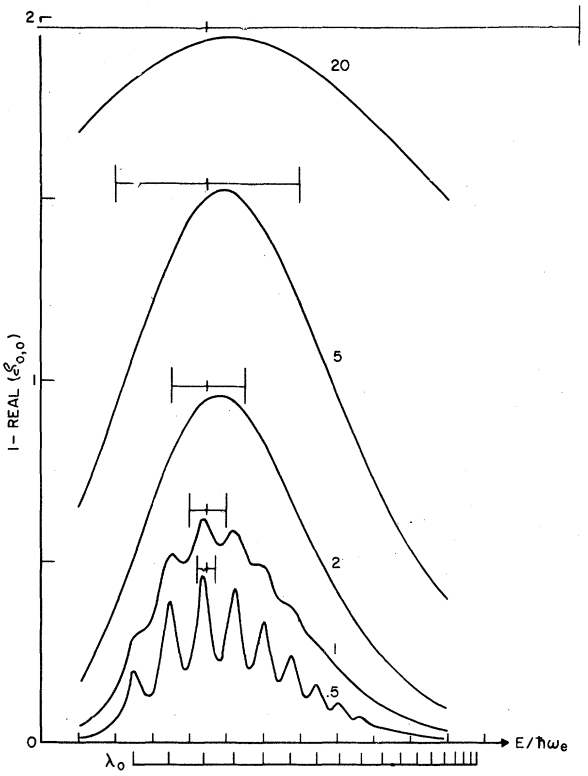


FIG. 6. Plot of $1 - \text{Real}\ (\mathcal{S}_{0,0})$ as a function of increasing width when only one electronic resonance $\lambda_0$ is present. If the matrix $A^0 = 1$ in Eq. (28), this represents a plot of the total cross section. The locations of the vibrational resonance series are shown at the bottom of the figure. The total width, $\Gamma_{\lambda_0}$ is the same for each electronic-vibrational resonance and is indicated by the bars over each curve. The numbers labeling each curve indicate these widths in units of the vibrational spacing $\hbar\omega_e$. The energy scale also is in units of $\hbar\omega_e$.

Figure 8 shows the real part of $\mathcal{S}_{0,0}$ for various combinations of electronic widths. In the lowest curve, corresponding to widths of $\frac{1}{8}$ and $\frac{1}{2}$ of the vibrational spacing for $\lambda_0$ and $\lambda_1$, respectively, we can begin to resolve the two electronic series. However, as the widths get progressively wider we approach the case of a single series of *narrow* resonances imbedded in a large background. The limiting behavior of the $\mathcal{S}$ matrix for two electronic series is obtained from Eq. (68). In the limit of small $\Gamma_\lambda$ we obtain (for $\lambda = 0,1$),

$$\mathcal{S}_{\alpha,\beta} \xrightarrow[\Gamma_\lambda \to 0]{} +\delta_{\alpha,\beta} + F_{\alpha,\nu} F_{\beta,\nu} \frac{(-i\Gamma_\lambda)}{E - \mathcal{E}_{\lambda,\nu} + i\Gamma_\lambda/2} \tag{70}$$

with the usual Breit-Wigner formula in the vicinity of each of the two series of resonances, $E = \mathcal{E}_{\lambda_0,\nu}$ and $E = \mathcal{E}_{\lambda_1,\nu}$ However for large $\Gamma_\lambda$ we obtain a single series of BW resonances with modified widths $\bar{\Gamma}_\nu$ and resonance energies $\bar{\mathcal{E}}_\nu$

$$\mathcal{S}_{\alpha,\beta} \xrightarrow[\Gamma_\lambda \to \infty]{} -\delta_{\alpha,\beta} - F_{\alpha,\nu} F_{\beta,\nu} \frac{(-i\bar{\Gamma}_\nu)}{E - \bar{\mathcal{E}}_\nu + i\bar{\Gamma}_\nu/2} \tag{71}$$

Notice however the changes in sign compared to Eq. (70). $\bar{\mathcal{E}}_\nu$ is the mean of $\mathcal{E}_{0,\nu}$ and $\mathcal{E}_{1,\nu}$ weighted by $\Gamma_{\lambda_1}$ and $\Gamma_{\lambda_2}$ while $\bar{\Gamma}_\nu$ depends on the spacings between the original resonances, and their respective widths.

$$\bar{\mathcal{E}}_\nu = (\mathcal{E}_{0,\nu}\Gamma_{\lambda_1} + \mathcal{E}_{1,\nu}\Gamma_{\lambda_2})/(\Gamma_{\lambda_0} + \Gamma_{\lambda_1}), \tag{72}$$

$$\bar{\Gamma}_\nu = 4\Gamma_{\lambda_0}\Gamma_{\lambda_1}(\mathcal{E}_{0,\nu} - \mathcal{E}_{1,\nu})^2/(\Gamma_{\lambda_0} + \Gamma_{\lambda_1})^3. \tag{73}$$

The overlap effect is shown more explicitly in Fig. 9 for the extreme case of $\Gamma_{\lambda_1} = 20$ and $\Gamma_{\lambda_0} = 5$. For comparison the cross sections which would be obtained if the two series were isolated are also shown. The arrows indicate the locations of the modified resonances. A similar presentation is made in Fig. 10 for the inelastic cross section $|\mathcal{S}_{0,1}|^2$. The change in the shape of the resonances in midseries is due to the changing sign of $F_{\nu,1}$.

Finally some mention should be made of effects which have been neglected in this study. We have only considered the case of one open electronic

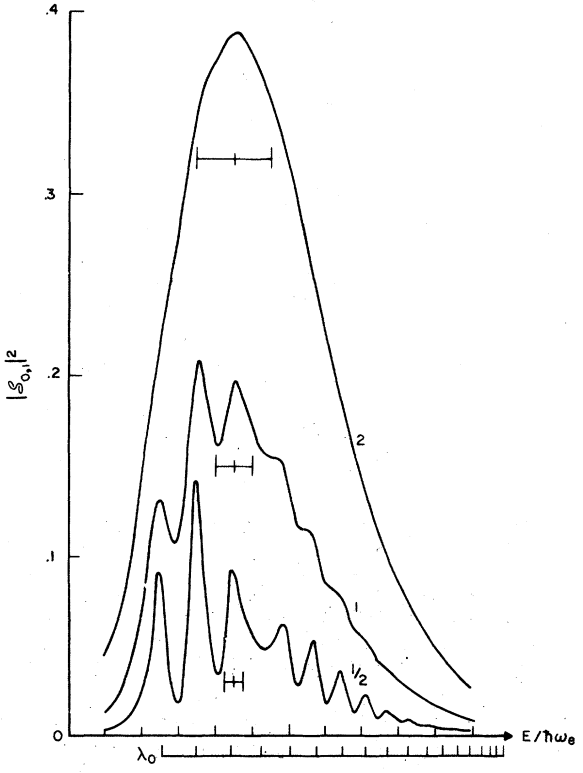


FIG. 7. Plot of $|\mathcal{S}_{0,1}|^2$ for the case presented in Fig. 6. If the $A^0$ matrix in Eq. (28) is diagonal, this represents a plot of the $\alpha = 0 \to \alpha = 1$ vibrational excitation cross section.

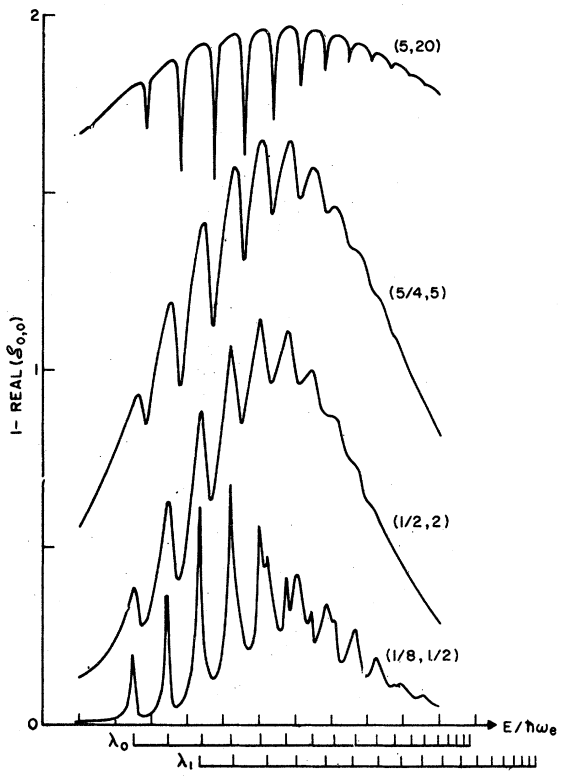


FIG. 8. Plot of 1 – Real $(S_{0,0})$ for various combinations of widths $(\Gamma_{\lambda_0}, \Gamma_{\lambda_1})$ when the two electronic resonances shown in Fig. 5 overlap. The locations of the vibrational resonances are shown at the bottom of the figure. The pair of numbers which label each curve indicate the widths $\Gamma_{\lambda_0}$ and $\Gamma_{\lambda_1}$, respectively, in units of the vibrational spacing $\hbar\omega_e$.

channel. Certainly in the case of electron-$H_2$ scattering other channels must be included. The effect of an $R$ dependent electron width must be considered, in which case the unusual feature of the $v_{n,\alpha}$ matrix being orthogonal will be destroyed. Lastly the assumption that all electronic resonances have the same vibrational structure must be relaxed, although it may not be unreasonable for a given Rydberg series of molecular resonance states.

## VI. SUMMARY AND CONCLUSIONS

There is a natural desire among scientists to relate experimental observations to intrinsic molecular properties of the system being studied, and thus the temptation to associate the location of each bump or oscillation in a photon or electron scattering experiment with some approximate eigenstate of the collision complex, or so-called resonance state is understandable. Further the breadth of the oscillation is often associated with the width of the resonance and is used as a measure of the configuration interaction between the resonance state and the accessible continuum states. However, these simple relationships are destroyed when adjacent resonances, which are imbedded in the same continua, overlap.

The present CI theory includes the effects of both inelastic potential scattering and the coupling of many resonances to many channels, and has been applied to various models representing atomic photoionization and electron molecule scattering. The effects of inelastic potential scattering have not been examined explicitly in terms of the models, but are fairly apparent from the theoretical expression in Eq. (28). Rather, emphasis has been given to the effects of overlapping resonances. A new parameter, the overlap matrix $\mathcal{O}$, has been introduced to measure the degree to which different resonance states overlap.

If $\mathcal{O} = \tilde{1}$ we say the resonances are *superimposed*, since they each couple to separate, mutually orthogonal continua, and they may be treated as single isolated resonances. As the total widths $\Gamma_n$ exceed the spacing between neighboring resonances the structure of the cross sections becomes unresolved (see Figs. 6 and 7). However, if $\mathcal{O} \neq \tilde{1}$, the resonances *overlap* and exhibit interference effects due to their mutual interaction with common continua. The striking feature of the overlap effect is

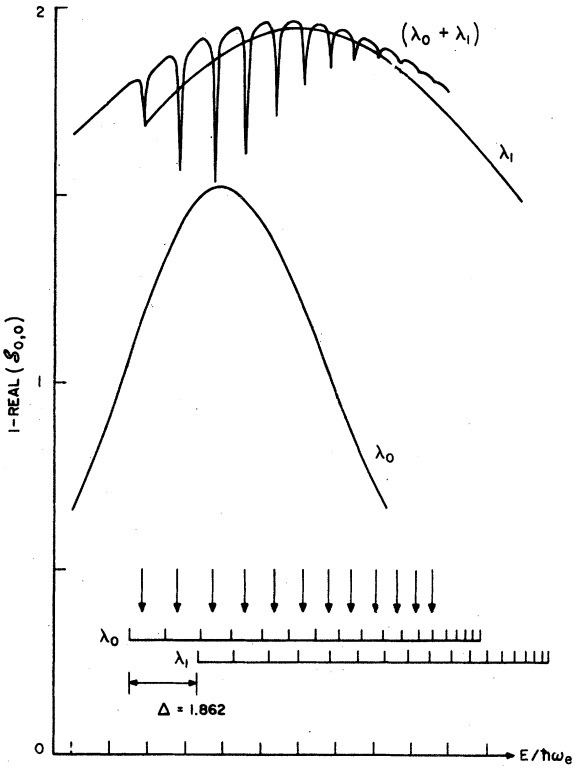


FIG. 9. Plot of 1 – Real $(S_{0,0})$ for $\Gamma_{\lambda_0}=5$ and $\Gamma_{\lambda_1}=20$ corresponding to the extreme case in Fig. 8. This curve is labeled $(\lambda_0+\lambda_1)$. Also shown are the expected curves $\lambda_1$ and $\lambda_2$ for the two electronic series if they were isolated, as in Fig. 6. The arrows at the bottom of the figure locate the positions of the Breit-Wigner resonances in the overlapping curve. The position and widths of the resonances are in quantitative agreement with Eqs. (72) and (73).

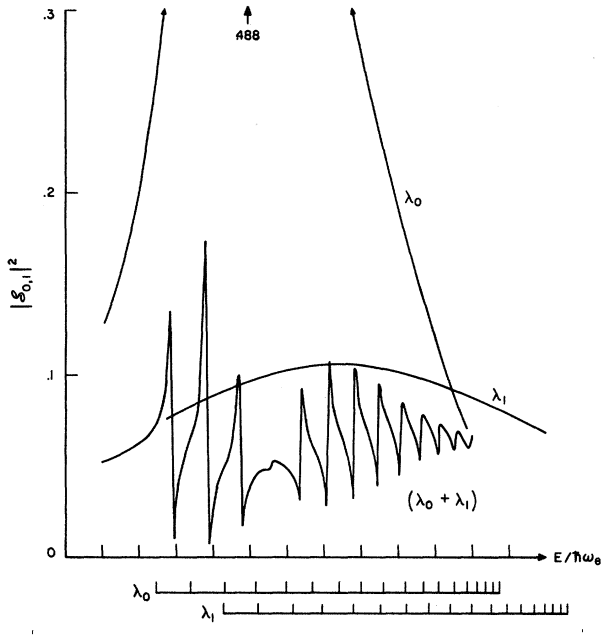


FIG. 10. Plot of $|S_{0,1}|^2$ for the case presented in Fig. 9.

that often the cross sections persist in oscillating between resonance positions even when the widths greatly exceed the spacings (Figs. 1,2,3,8,9, and 10). Thus the "observed" widths which appear never exceed the spacings between those resonances which overlap. By varying the degree of overlap the "observed" widths vary and bear no simple relationship to $\Gamma_n$ (see Figs. 2 and 3).

In conclusion, we find that to properly characterize a resonance we must know not only its resonance energy $E_n$, and its partial widths $\Gamma_{n,\alpha} = 2\pi V^2_{n,\alpha}$ into each accessible channel, but also the phase of the CI matrix elements $V_{n,\alpha}$. This is necessary to obtain $\Theta$ in Eq. (43). Thus from a theoretical viewpoint there is an important need to determine $V_{n,\alpha}$ in addition to solving the more trivial "eigenvalue" problem. And from the experimental viewpoint, both differential and inelastic cross sections into all accessible channels are needed to further characterize the resonances.

## ACKNOWLEDGMENTS

The author is grateful to J. Cooper and U. Fano for their helpful suggestions and especially to M. Krauss for his stimulating and encouraging discussions.

---

*This research was supported in part by the Advanced Research Projects Agency of the Department of Defense under the Strategic Technology Office.

[1]U. Fano, Phys. Rev. 124, 1866 (1961).

[2]F. H. Mies and M. Krauss, J. Chem. Phys. 45, 4455 (1966).

[3]H. Feshbach, Ann. Phys. (N. Y.) 43, 410 (1967).

[4]J. M. Blatt and L. C. Biedenharn, Rev. Mod. Phys. 24, 258 (1952).

[5]Primed matrices will be used to designate an implicit dependence $(E, E')$ while the same matrix without the prime implies $E' = E$, or $(E, E)$.

[6]See U. Fano and F. Prats, J. Natl. Acad. Sci. India A33, 553 (1963) for a discussion of the normalization for the standing wave representation and the resultant expressions for the reactance and scattering matrices.

[7]For a discussion of the transition amplitude see A. Messiah, Quantum Mechanics (John Wiley & Sons, Inc., New York, 1965), Vol. II, p. 1007. Recall that Eqs. (8) and (31) are for a specific $\vec{J}$, $\vec{S}$. If differential cross sections are required, a linear combination of the continua $\Psi_\alpha^-$ may be required in Eq. (31).

[8]U. Fano and J. W. Cooper, Phys. Rev. 137, 1364A (1965).

[9]Equation (48) in combination with Eq. (28) yields Feshbach's Eq. (34) for a single channel (see Ref. 3).

[10]Often a superposition of isolated resonances is used to parametrically represent the experimental observations (see Ref. 11),

$$\sigma = \sigma_b' + \sum_{n'} \sigma_{a,n'} [(q_{n'}/\epsilon_{n'}) + 1]^2/(1+\epsilon_{n'}{}^2)$$

where

$$\epsilon_{n'} = 2(E - \mathcal{E}_{n'})/\Gamma_{n'}$$

Obviously the set of parameters $\{\Gamma_{n'}, q_{n'}, \mathcal{E}_{n'}\}$ one obtains from such a fit have no immediate relationship to the intrinsic molecular properties $\{\Gamma_n, q_n, \mathcal{E}_n\}$ of Eq. (50), unless the widths $\Gamma_n$ are truly narrow and hence the resonances $\mathcal{E}_n$ are isolated. It is not ever apparent that this equation can analytically fit the $E$ dependence of Eq. (50).

[11]B. W. Shore, Rev. Mod. Phys. 39, 439 (1967).

[12]E. P. Wigner, Ann. Math. 53, 36 (1951).

[13]This expression from Ref. (8) is not quite correct for small $p$. See U. Fano and J. Cooper, Rev. Mod. Phys. (to be published). It should equal $2(p - p_\lambda{}^*)^{-3}$, however it has no significant effect on the model calculations.

[14]$\mathcal{K}$ is a bordered matrix for this case. It was truncated at $\Omega = 18$, and diagonalized numerically. This introduces the overlapping between the first 17 resonances. Beyond $\Omega = 18$ the off-diagonal terms are extremely small, i.e., the autoionization widths are small compared to the Auger widths, and overlapping effects are negligible ($\Theta < 0.01$).

[15]Auger processes have been observed in the far uv in Kr and Xe. Our model was designed with the $^2D_{5/2}\, np$ Rydberg series of Xe in mind (begins at 190.41Å). However, for purposes of emphasizing the overlapping effects, the contribution of "autoionization" widths are exaggerated, and the results in Fig. 4 do not reproduce the true Xe spectra. See K. Codling and R. P. Madden, Phys. Rev. Letters 12, 106 (1964) and A. P. Lukirskii, T. M. Zimkins, and I. A. Brytov, Bull. Acad. Sci. USSR, Phys. Ser. 28, 681 (1964). [English transl.: Izv. Akad. Nauk SSSR Ser. Fiz. 28, 681 (1964)].

[16]J. C. Y. Chen, Phys. Rev. 146, 61 (1966); J. C. Y. Chen, J. Chem. Phys. 40, 3507 (1964) 40, 3507 (1964).